SINUS AESTUUM: THE PERVASIVE UNSAMPLED *OTHER* LUNAR SPINEL LITHOLOGY. C. M. Pieters[1,2] and J. M. Sunshine[3], [1]DEEPS, Brown Univ., Providence RI 02912 (carle_pieters@brown.edu), [2]Planetary Science Institute, Tucson, AZ, [3]Univ. of Maryland, Dept. of Astronomy, College Park MD, 20742

Introduction: The Moon Mineralogy Mapper (M^3) enabled the discovery of an unsampled but widely distributed Mg-spinel anorthosite rock type found in crustal terrains across the lunar surface [1,2]. Mg-spinel is readily recognized by the presence of a prominent absorption near 2 μm in anorthosite terrain. However, when the spinel composition is Fe-rich, in addition to a distinct absorption near 2 μm, it is also relatively dark. Terrain containing significant Fe-rich spinel appear dark at visible wavelengths in remote sensing measurements. Such a Fe-rich spinel composition has been recognized to dominate one of the regional pyroclastic deposits on the lunar nearside [**Figure 1**], specifically at Sinus Aestuum [3,4,5,6,7]. Although pyroclastic deposits have been directly sampled at Apollo 17 (Fe,Ti-rich 'orange glass' and ilmenite-rich 'black beads'), the Sinus Aestuum deposits clearly exhibit a distinct mineral composition with Fe-rich spinel, implying a different source region within the lunar mantle.

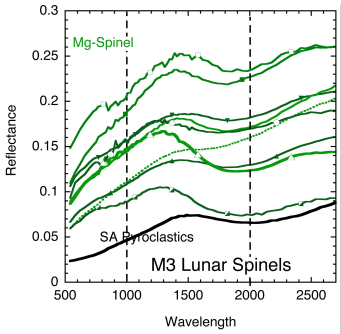

Figure 1. Summary of spinel-dominated lithologies observed on the Moon with M^3. Most are crustal Mg-rich spinel bearing areas (shown in green) [2]. The darkest is for the pyroclastic deposits found across Sinus Aestuum containing Fe-rich spinel.

Unfortunately, neither of these prominent, but very different, spinel-bearing lunar lithologies have been sampled making it difficult to investigate their character and understand their origin. The distinct Sinus Aestuum pyroclastic material, located on the central nearside, presents an excellent and scientifically rich target for automated lunar sample return.

Context: The regional context of the dark Sinus Aestuum pyroclastic deposits as observed with M^3 is shown in **Figure 2** [2] and spectra are shown in **Figure 3**. The region is south of Rima Bode and southeast of Copernicus on the lunar nearside. The western half of the scene exhibits crater rays which originated from Copernicus emplaced on mare basalt. Superimposed small craters across the scene expose relatively unweathered local lithologies, color coded here as red (pyroxene-rich basalts) and green (spinel-rich pyroclastic material).

Note that ***SA1 soil*** represents local well developed (undisturbed) Sinus Aestuum (pyroclastic) soil that has accumulated local space weathering since its deposition (billions of years ago). In contrast, **SA-2** is thought to represent relatively unweathered pyroclastic deposits exposed within a medium-sized crater. All other spectra are associated with craters (some very subdued) of indeterminate age. **SA-8** provides an example of local basalt exposed by a relatively fresh crater in the mare to the west of the pyroclastic deposits.

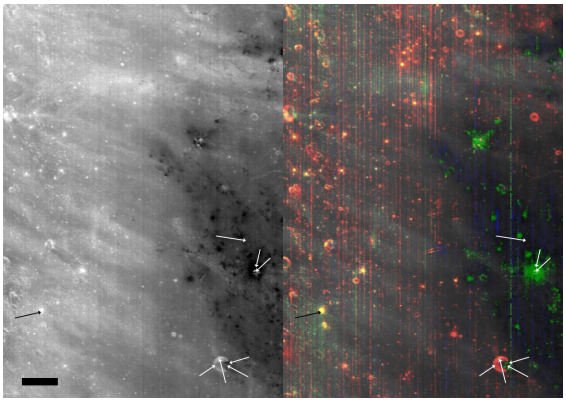

Figure 2. Western Sinus Aestuum pyroclastic terrain as viewed with M^3 [2]. [left] Reflectance image at 700 nm. [right] Color composite rock type image superimposed on reflectance (red/yellow areas are pyroxene-rich; green areas are spinel-rich). Arrows indicate location of representative M^3 spectra shown in Figure 3. Scale bar is 10 km. The ~5 km crater in lower right is Schröter D.

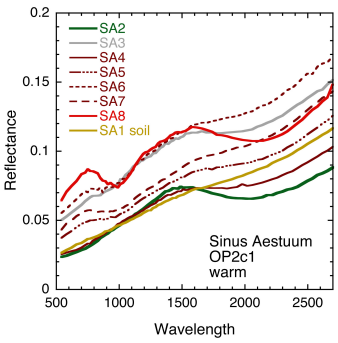

Figure 3. Spectra for eight areas indicated in Figure 2 with arrows. Starting with arrow orientation down near vertical and proceeding clockwise: SA-2, SA-3, SA-4, SA-5, SA-6, SA-7, SA-8, SA-soil.

Understanding the compositional details and origin of these unsampled pyroclastic deposits on the lunar nearside is limited with remote sensing capabilities. *On the other hand, comprehensive analysis would provide a valuable new link to the lunar mantle. Their easy access and relatively low rock abundance make them a very attractive target for robotic sample return.*

References: [1] Pieters, C. M., et al. (2011), *JGR*, 116; [2] Pieters, C. M. et al. (2014), *Am. Min.* 99, 1893. [3] J. M. Sunshine et al. (2010), LPSC 41, #1508; [4] S. Yamamoto et al., (2013), *GRL*, 40, 4549-4554; [5] J. M. Sunshine et al. (2014) LPSC 45, #2297. [6] S. Li and R. Milliken (2017) LPSC48, 2476. [7] C. Weitz et al. (2017) *JGR-P* 122 2013.